Rapid Analysis of Single Droplets of Lanthanide−Ligand Solutions by Electrospray Ionization Mass Spectrometry Using an Induction-Based Fluidics Source

Gary S. Groenewold,*,† Andrew D. Sauter, Jr.,‡ and Andrew D. Sauter, III‡

†Idaho National Laboratory, 2351 North Boulevard, Idaho Falls, Idaho 83415-2208, United States
‡Nanoliter, LLC, 217 Garfield Drive, Henderson, Nevada 89074, United States

S *Supporting Information*

ABSTRACT: Electrospray ionization mass spectra of lanthanide coordination complexes were measured by launching nanoliter-sized droplets directly into the aperture of an electrospray ionization mass spectrometer. Droplets ranged in size from 102 nL to 17 nL, while metal concentrations were 293 μM. The sample solution was delivered to a source capillary by a nanoliter dispenser at a rate of 21 nL/s, and droplets were ejected from the capillary by pulsing a potential onto the capillary. The end of the capillary was situated in front of the mass spectrometer and aimed directly at the aperture. The period and power of the electrical pulse was controlled by a digital energy source. The intensity of the extracted ion time profiles from the experiment showed reproducible production

of lanthanide nitrato-anion complexes (Ce, Tb, and Lu). The integrated ion intensities of the complexes were reproducible, having relative standard deviations on the order 10% for anions, and 10−30% for cations. The integrated ion intensities were proportional to the droplet size, and the response was linear from about 100 to 650 pmol. However, the intercept is not zero, indicating a nonlinear response at lower analyte quantities or droplet sizes. Cation complexes were generated in separate experiments that corresponded to lanthanide nitrate ion pairs coordinated with the separations ligand octyl,phenyl,(N,N-diisobutylcarbamoyl)methylphosphine oxide (CMPO). Experiments showed a preference for formation of CMPO complexes with Ln^{3+} having larger ionic radii. The relative standard deviation values of the cation abundance measurements were somewhat higher for the more highly coordinated complexes, which are also less stable. The mass spectral quality was high enough to measure the ratios of the minor isotopic ions to a high degree of accuracy. The approach suggests that the methodology has utility for analysis of solutions where the sample quantity is limited, or where the sampling efficiency of a normal ESI source is limiting on account of hazards derived from the sample solution.
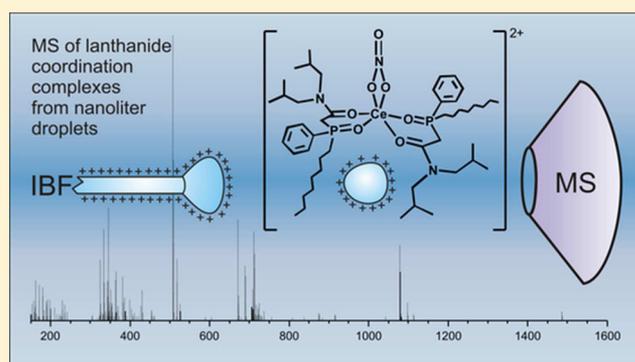
Over the past 10−15 years, droplets have found increasing utilization in analytical chemistry, particularly for sample collection. A microliter-sized droplet of a nonmiscible fluid formed on the end of a syringe or capillary can be inserted into a sample liquid or headspace, whereupon partitioning of analyte into the droplet will occur. The droplet can be retracted and then analyzed directly using GC or a comparable technique.[1] Recently, even smaller droplets have been used for accurately and reproducibly forming samples for MALDI analyses. A technique referred to as induction-based fluidics (IBF) has been used to form and shoot droplets of ionic liquids having volumes as small as 20 nL at MALDI targets, and subsequent analysis of these targets resulted in higher sensitivity and better reproducibility compared to direct deposition of microliter volumes.[2] IBF functions by forming a nanoliter droplet on the end of a Gaussian surface, such as a nonconducting capillary. The capillary is connected to an electrical source, and application of a pulse results in induction of surface charge on both the capillary and on the surface of the droplet. The

magnitude of the induced charge is correlated with surface area of the droplet[3] and causes repulsion between the capillary tip and the droplet, launching the droplet with sufficient energy to traverse the distance between the capillary and a target. Related approaches were first reported by Lord Raleigh[4] and commercialized in the 1950s.[5] In the MALDI analysis of bradykinin, nanoliter targets generated using IBF displayed significantly improved response.[2] Similarly, MALDI analyses of polymer targets made using IBF had notably enhanced intensity and signal-to-noise, likely on account of increased surface concentration of polymer analyte compared to microliter droplet deposition and possibly because of field-enhanced crystallization.[6] The improved sensitivity and precision motivated the use of IBF to prepare samples of single neurons

for peptide analysis using MALDI.[7] IBF has also been used to deposit nanoliter droplets of glycerol onto surfaces, where the glycerol solubilizes analytes, enabling measurement using liquid secondary ion mass spectrometry with significantly improved sensitivity.[8]

Because IBF accurately transfers solutions from a sample delivery device to a desired target location, it also has application for improving the efficiency of sample transfer to electrospray ionization (ESI) mass spectrometers.[9] ESI revolutionized analytical chemistry, enabling mass spectrometric analysis of a truly vast array of chemicals,[10] including metal complexes.[11] However, a drawback is that the large majority of the sample is not transferred into the mass spectrometer aperture. This is a consequence of the fact that charged droplets produced by the electrospray capillary Coulombicly repel each other and adopt trajectories that are significantly deflected from the aperture axis. The majority of the solutes in these droplets will not be sampled but will instead be deposited on the outside of the ESI source. In instances where the sample is limited, or where the sample has hazardous characteristics, such deposition is undesirable, and so there is a need for an alternative means for more accurately transferring droplets into the mass spectrometer aperture. The possibility of using IBF to achieve a higher delivery efficiency stems from the fact that IBF launches sample droplets in a one-at-a-time fashion; accordingly droplet−droplet repulsion is not a factor, and droplet trajectories can be aligned with the aperture axis with a high level of accuracy. Preliminary studies had shown the feasibility of using IBF for ESI analysis of single droplets containing a range of metals, pharmaceuticals, and peptides.[9a,b]

In the present experiments, an IBF source was aligned with the aperture of an ESI mass spectrometer, and the instrument was used to analyze nanoliter-sized droplets of solutions containing lanthanide (Ln) nitrates and an organic ligand used in solvent-extraction processes for metal separations, namely octyl,phenyl,(*N,N*-diisobutylcarbamoyl)methylphosphine oxide or CMPO. The motivation for analyzing this particular type of sample is that lanthanide recovery and utilization are topics of increasing importance as a result of their scarcity and thus fast efficient means for measuring speciation are needed. The analysis of lanthanide metals is also important in solutions generated by nuclear fuel recycling, which tend to have high HNO_3 concentrations. These issues have motivated a number of ESI-MS studies of lanthanide-containing solutions.[12] One particularly challenging problem is separation of the trivalent transuranium elements from the lanthanide fission products, and CMPO has been extensively studied as a possible complexant for use in this separation.[13] The importance of CMPO-type ligands motivated Crowe and colleagues to study lanthanide (Ln) coordination complexes of the bis-phenyl, (*N,N*-diisobutylcarbamoyl)methyl-CMPO derivative using ESI-MS.[14] ESI of nitric acid-containing solutions produced mainly $[Ln(NO_3)_2(CMPO)_2]^+$, and collision-induced dissociation studies showed that HNO_3 is eliminated from these complexes with decreasing energy as one proceeds across the 4f period. This observation was interpreted in terms of stronger CMPO binding/weaker NO_3^- binding as the ionic radius decreases on going from La^{3+} to Lu^{3+}. These results highlighted the rich level of information that can be garnered from ESI-MS analyses of these systems, which in operating processes would be quite radioactive. These issues and prior results provide the impetus for investigating sample introduction methodologies having higher transmission efficiencies.

■ EXPERIMENTAL SECTION

The induction-based fluidics device was procured from Nanoliter LLC (217 Garfield Drive, Henderson, NV 89074); it consists of a DC power supply coupled to a digitally controlled pump that was that was operated at a rate of 21 nL/s. The droplets were ejected by application of a programmed electrical pulse or wave applied anywhere from a few hundred milliseconds to several seconds after droplet accumulation was initiated. The electrical pulse or wave was supplied by a patent-pending nanoLiter Cool Wave programmable DC power supply to apply a DC wave or pulse with a value, form, and duration that are of sufficient field strength and duration to effect single droplet launch to the mass spectrometer from a Gaussian surface, in this case a capillary.[15a,b] This capillary was either a 150 μM o.d./50 μM i.d. section of fused silica capillary (~1 cm in length) or was a glass capillary joined to a nanoLiter Cool Wave microliter syringe where a glass sleeve was employed to compression fit the parts together. A standard Hamilton capillary syringe was also used, and both of these apparati worked equally well. The dispenser was aimed directly at the aperture of the mass spectrometer and was situated such that the end of the capillary was on the order of 3 mm from the aperture entrance. Any closer than that resulted in significantly poorer signal intensities, presumably because the drop had inadequate evaporation time prior to entering the sampling capillary downstream of the sampling aperture.

A Bruker Daltonics (Billerica, MA) MicrOTOF-QII electrospray ionization mass spectrometer was used for these experiments. Normally, the instrument consists of an ESI source that is connected via a transfer capillary to a quadrupole mass analyzer, a collision cell, and a time-of-flight mass analyzer. This combination enables high mass resolution/high mass accuracy mass measurement sufficient for assigning elemental composition, and collision-induced dissociation−mass spectrometry/mass spectrometry experiments. Mass resolution was on the order of 8000 $m/\Delta m$ (10% valley definition, Figure S1, Supporting Information), and mass accuracy was generally within 6 ppm, operating with an external calibration against the tuning mixture ESI-L (Table S1, Supporting Information, Agilent Technologies, Santa Clara, CA), and improved to <1 ppm when files were calibrated internally (Table S2, Supporting Information).

In the present experiment, the ESI source was removed, which enabled the IBF capillary to be situated in front of the sampling aperture. The mass spectrometer was operated using the standard Bruker settings for negative electrospray ionization (Table S3, Supporting Information), with the exception that the number of microscans averaged per scan was reduced from 5000 to 500, which enabled spectral acquisition at a rate of 10 Hz. This was necessary to keep up with the rapid intensity changes caused by the droplet solutes traversing the mass spectrometer. The dry gas temperature at the spectrometer aperture was maintained at 80 °C. This value is significantly less than that normally used, but at higher values, rapid evaporation of the drop occurred at the capillary, which interfered with the process of repelling the drop into the aperture. The drying gas flow rate was set at 4 L/min.

Solutions of cerium, terbium, and lutetium nitrate salts were gravimetrically prepared to a concentration of 2.93 mM in H_2O. A volume of 100 μL of these solutions was diluted by the addition of 200 μL of an ethanolic CMPO (Strem Chemicals Inc., Newburyport, MA) solution with a concentration of 580

μM, and 700 μL of acetonitrile. CMPO does not show up in the negative ion mode. The final concentrations were 293 μM lanthanide and 116 μM CMPO.

■ RESULTS AND DISCUSSION

Anion Analyses. Analysis of a single droplet of a solution containing Ce, Tb, Lu, and CMPO furnished a negative ion mass spectrum containing the tetrakis-nitrato complexes of the three lanthanide metals $[Ln(NO_3)_4]^-$ (Figure 1). In addition, a
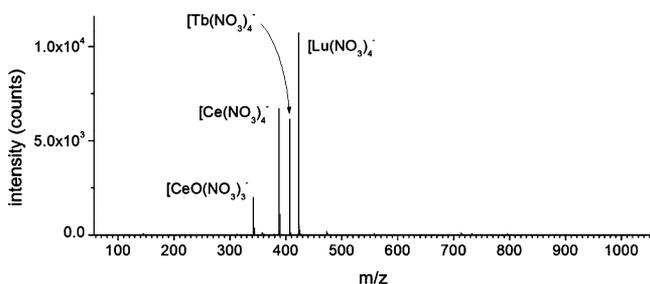
Figure 1. Negative ion mass spectrum of a single 17 nL droplet of a lanthanide nitrate solution (293 μM).

lower abundance ion was identified as $[CeO(NO_3)_3]^-$ that arises from oxidation of the cerous cation. This could occur in the standard solution or in the electrospray capillary, but the location where this is occurring has not been identified.

Substituting the IBF source for the standard ESI source did not compromise the function of the TOF mass spectrometer. The accurate m/z values measured for the nitrato clusters were within a few tenths of a part per million (Table S2), and the relative abundances of ions containing minor isotopes of the Ln metals, oxygen, and nitrogen were very close to theoretical values (Figure 2; Table S4, Supporting Information). In the isotopic envelope of the $[Ce(NO_3)_4]^-$ complex, the most abundant ion is at nominal m/z 388, which primarily corresponds to $[^{140}Ce(NO_3)_4]^-$, and an abundant isotopic ion is seen at m/z 390, which is principally $[^{142}Ce(NO_3)_4]^-$. The relative abundances of these two ions and those containing

the minor isotopes ^{136}Ce and $(^{142}Ce + {}^{15}N)$ at m/z 384 and 391 were measured within 10% percent of their theoretical values. Isotopic ions containing ^{138}Ce and $(^{140}Ce + {}^{15}N)$ at m/z 386 and 389 were measured at values 83% and 17% higher than theoretical. The apparently inaccurate values could be due to higher energy, low mass tails of the very abundant ions one mass unit higher at m/z 388 and 390; however, the exact cause has not yet been determined. Terbium is monoisotopic, with the most abundant peak in the isotopic envelope of $[Tb(NO_3)_4]^-$ is at nominal m/z 407, with minor isotopic ions one and two mass units higher (m/z 408 and 409) that contain principally ^{15}N and ^{18}O, respectively. The minor isotopic ions are measured within 16% and 7% relative to their theoretical values, with poorer accuracy observed in the ion proximate to the major isotopic peak at m/z 407. Lutetium has a major isotopic ion at m/z 423 in the $[Lu(NO_3)_4]^-$ isotopic envelope, with a minor isotopic peak at m/z 424 that mainly contains ^{15}N, and an isotopic peak at m/z 425 that arises from ^{18}O. The relative abundances of the minor isotopes in the Lu complex are within 6% and 3% of their theoretical abundances, respectively. These results suggest that the abundances of the minor isotopic ions could be measured with good accuracy from the single droplet data, particularly if a mass analyzer with better baseline discrimination was employed.

Reproducibility was evaluated using the digital energy source, which applies potential to the droplet capillary at a predetermined rate. In these experiments, the pump was operated to deliver sample solution at a rate of 21 nL/s. The rate at which the potential was pulsed was initially 0.204 Hz, which resulted in ejection of a drop from the end of the capillary every 4.89 s. This is seen beginning at 180 s in the temporal infusion profile shown in Figure 3. The pulse rate was then speeded up to 0.326 Hz, which produced a drop every 3.07 s (section beginning at 275 s). The pulse rate was again increased to 1.23 Hz, producing a drop every 0.813 s (beginning at 362 s). The sequence was then reversed, which demonstrated the ability to systematically decrease the rate of droplet formation. The mass spectra acquired for the drops produced by the faster pulse rates were identical to those produced by the slowest pulse rate.

We next evaluated the precision of the droplet delivery at the three different droplet delivery rates. Because the pump was running continuously, the drop volume and the quantity of solute varied linearly with the number of seconds required for formation of each drop. The precision of the mass spectrometric ion signal from the droplets was calculated (as percent relative standard deviation) for the total ion current and extracted ion currents for the major isotopic peaks of the three $[Ln(NO_3)_4]^-$; values ranged from 7% to 13% (Table S5, Supporting Information). When the integrated peak areas were plotted versus the moles of lanthanide in each droplet, a linear relationship was observed for all four ions of interest, from about 100 to 650 picomol/droplet (Figure 4). The plots do not go through the intercept, which may be because the sample has not cleared the mass spectrometer before the next drop is delivered. This phenomenon is most easily observed in the ion profiles of the drops formed at the rate of 1.23 Hz, where the extracted ion intensities only decrease to about 30% of their peak intensity before the next drop is delivered. On the other hand, the trend indicated by the MS peak intensities from the 0.326 and 0.204 Hz droplets also indicates a nonzero intercept, and in these cases, the peak profiles clearly do return to zero. An alternative explanation might be that the plot of the peak

Figure 2. Comparison of abundances of minor isotopes with theoretical values. Left, $[Ce(NO_3)_4]^-$ isotopic ions. Right, $[Tb(NO_3)_4]^-$ and $[Lu(NO_3)_4]^-$ isotopic ions. Filled circles are averages of five droplets, with one standard deviation error bar. Open diamonds are theoretical values for the isotopic ions.
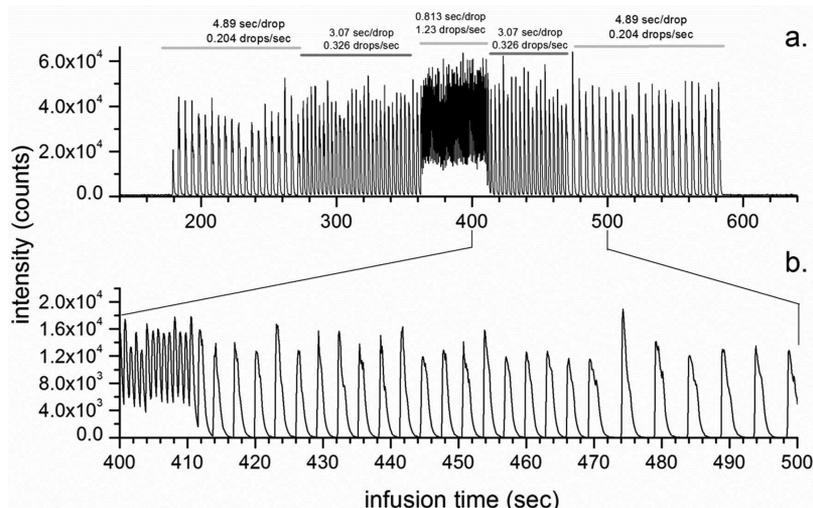
Figure 3. Infusion profiles of a series of individual droplets. (a) Total ion profile, showing five different frequency regimes. (b) Extracted ion profile of m/z 422.9, $[Lu(NO_3)_4]^-$ from 400 to 500 s.
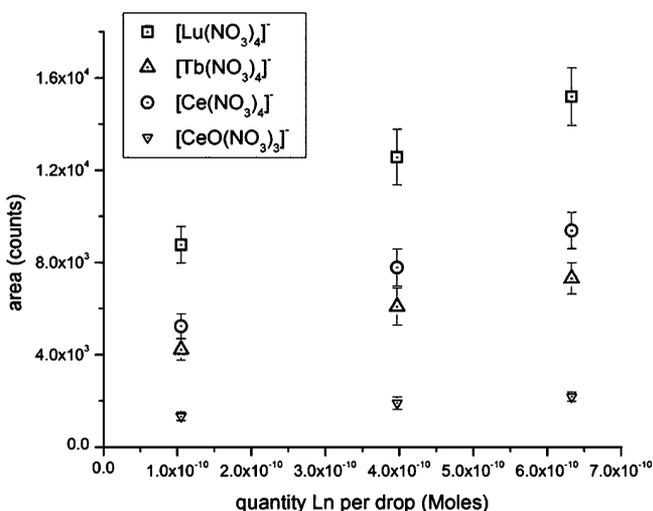
Figure 4. Areas of extracted anion profiles versus moles of Ln per drop.

areas versus droplet solute quantity may have a partially logarithmic character, which would mean that solutes are more sensitively detected when the total quantity of solute is lower.

This explanation is supported by the partially truncated peak profiles discussed below and suggests efficiency of ion formation from solutes in the concentration/droplet size ranges used in these experiments compared to lower concentrations or droplet sizes.

The mass of metal solute in the droplets was on the order of a few hundred picograms, and the signal-to-noise and intensity levels of the mass spectral and infusion profile peaks suggested that detection of smaller quantities is achievable. A close examination of the infusion profile peaks reveals a somewhat truncated peak top that suggests saturation of the mass spectral response, a conclusion consistent with the delivery of all of the analyte over a very short time frame. This in turn suggests that measurement of lower concentrations, smaller analyte volumes, or using faster MS duty cycles would be feasible, and that detection limits may well be in the low picogram range.

Cation Analyses. The cation analyses of lanthanide nitrate solutions are significantly more complex than their negative counterparts, in part because there are multiple, neutral nucleophilic components in solution capable of participating in positively charged coordination complexes: these include NO_3^-, CMPO, and acetonitrile (Figure 5). Ion compositions were made on the basis of accurate m/z measurements (Table 1), which in general were within 5 ppm of the theoretical
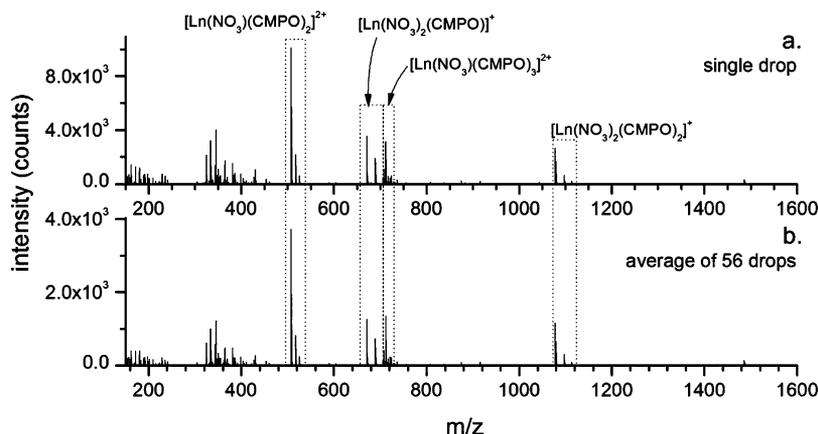
Figure 5. Positive ion spectra of a solution of Ce, Tb, and Lu nitrates with CMPO.

Table 1. Cation Complexes Observed in the Mass Spectrum of a Single Droplet of Ce^{3+}, Tb^{3+}, and Lu^{3+} Nitrates (293 mM) with CMPO (116 mM)

composition	theoretical m/z	measured m/z	ppm error
$[Ce(NO_3)(CH_3CN)_3]^{2+}$	162.4859	162.4859	0.00
$[Tb(NO_3)(CH_3CN)_3]^{2+}$	171.9959	172.0018	34.
$[Lu(NO_3)(CH_3CN)_3]^{2+}$	180.0036	180.0035	−0.56
$[Ce(NO_3)(CMPO)(CH_3CN)]^{2+}$	325.1070	325.1063	−2.2
$[Tb(NO_3)(CMPO)(CH_3CN)]^{2+}$	334.6170	334.616	−3.0
$[Lu(NO_3)(CMPO)(CH_3CN)]^{2+}$	342.6247	342.6213	−9.9
$[Ce(NO_3)(CMPO)(CH_3CN)(H_2O)]^{2+}$	334.1123	334.1124	0.30
$[Tb(NO_3)(CMPO)(CH_3CN)(H_2O)]^{2+}$	343.6222	343.6213	−2.6
$[Lu(NO_3)(CMPO)(CH_3CN)(H_2O)]^{2+}$	351.6300	351.6269	−8.8
$[Ce(NO_3)_2(CH_3CN)_2]^{+}$	345.9336	345.9337	0.29
$[Tb(NO_3)_2(CH_3CN)_2]^{+}$	364.9535	364.9518	−4.7
$[Lu(NO_3)_2(CH_3CN)_2]^{+}$	380.9690	380.9682	−2.1
$[Ce(NO_3)(CMPO)_2]^{2+}$	508.2414	508.2411	−0.59
$[Tb(NO_3)(CMPO)_2]^{2+}$	517.7513	517.7526	2.5
$[Lu(NO_3)(CMPO)_2]^{2+}$	525.7591	525.7594	0.57
$[Ce(NO_3)_2(CMPO)]^{+}$	671.1758	671.1755	−0.45
$[Tb(NO_3)_2(CMPO)]^{+}$	690.1957	690.1961	0.58
$[Lu(NO_3)_2(CMPO)]^{+}$	706.2112	706.2117	0.71
$[Ce(NO_3)(CMPO)_3]^{2+}$	711.8891	711.8894	0.42
$[Tb(NO_3)(CMPO)3]^{2+}$	721.3990	721.3965	−3.5
$[Lu(NO_3)(CMPO)_3]^{2+}$	729.4067	729.4087	2.7
$[Ce(NO_3)_2(CMPO)_2]^{+}$	1078.4712	1078.4711	−0.09
$[Tb(NO_3)_2(CMPO)_2]^{+}$	1097.4911	1097.4891	−1.8
$[Lu(NO_3)_2(CMPO)_2]^{+}$	1113.5065	1113.5062	−0.27

values; several ions displayed poorer accuracy which was attributed to unresolved doublets or low ion intensity which precluded accurate centroiding. The positive ESI mass spectra are complicated by the fact that 1+, 2+, and 3+ ions can be formed, a consequence of the 3+ oxidation state of the lanthanide cations. The most abundant ions in the mass spectrum are the 2+ complexes $[Ln(NO_3)(CMPO)_n]^{2+}$ ($n = 2$, 3, 4); for example, the Ln = Ce, $n = 2$ complex accounts for the base peak at m/z 508.24 (Figure 6). Tris-CMPO complexes are
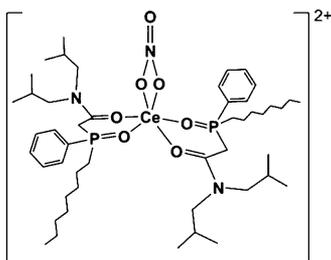
Figure 6. $[Ce(NO_3)(CMPO)_2]^{2+}$ structure.

also abundant, while tetrakis-CMPO complexes are formed at low abundance. Doubly charged ions complexed with acetonitrile are formed, but these are in much lower abundance, as expected given the much lower nucleophilicity of the acetonitrile molecules. The most abundant singly charged complexes are composed of Ce^{3+} and two NO_3^- with one, two, or three CMPO ligands. Singly charged complexes without CMPO contain acetonitrile instead, but these are much lower in abundance.

The digital energy source was used in these experiments to repetitively deliver 104 nL droplets to the TOF mass spectrometer (Figure 7). The quality of a mass spectrum
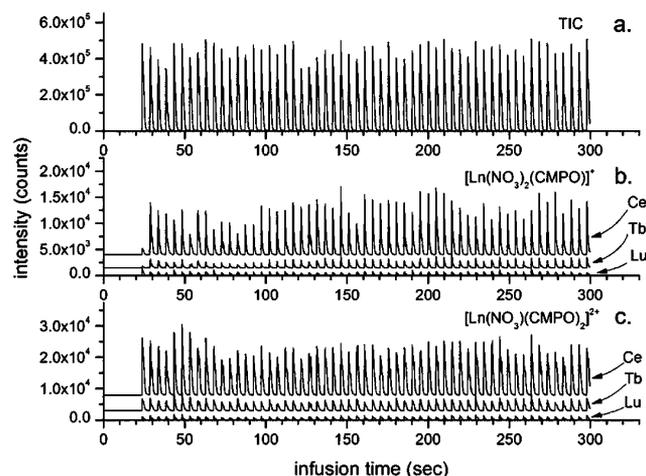
Figure 7. Positive ion profiles generated by individual drops. (a) Total ion current. (b) Singly charged complexes, $[Ln(NO_3)_2(CMPO)]^+$. (c) Doubly charged complexes, $[Ln(NO_3)(CMPO)_2]^{2+}$. The Ce and Tb profiles are offset from the baseline.

generated for an individual droplet was nearly identical to that generated by averaging 56 droplets (Figure 5), which indicated that a single droplet was sufficient to characterize the solution. Precision was evaluated by calculating percent relative standard deviation values (%RSD), which for the total ion current was 8.6% (Table S6, Supporting Information). The %RSD values for the complexes containing a total of three ligands were in the range of 10−15%; however, in the most coordinationally crowded complexes, higher values on the order of 20−30% were calculated. We believe that this reflects the sensitivity of the more highly coordinated complexes to small changes in droplet size or temperature although more study will be needed to further understand variability and refine precision.

The mixed metal experiments suggest that the relative affinity of the cations for CMPO in the droplets decreases in the order Ce^{3+} > Tb^{3+} > Lu^{3+}. Fractional ion abundances (fa) were calculated by dividing the integrated ion intensity (i) for a given metal coordination complex by the sum of intensities of all three metal (M) complexes having the same composition, i.e., for $[Ce(NO_3)(CMPO)_2]^{2+}$,

$$fa[Ce(NO_3)(CMPO)_2]^{2+}$$
$$= i[Ce(NO_3)(CMPO)_2]^{2+}/$$
$$\sum (i[Ln(NO_3)(CMPO)_2]^{2+})$$

For the 1+ complexes containing CMPO, Ce^{3+} fa values ranged from ~0.6 to 0.8, compared to values of 0.2−0.3 for Tb^{3+}, and <0.1 for Lu^{3+} (Figure 8). The same trend was seen for acetonitrile-containing complexes without CMPO, although the differences were not quite as great. For the 2+ complexes, a comparison of the metals showed that even more pronounced differences in fa values, with Ce^{3+} accounting for ~0.8, Tb^{3+} < 0.2, and Lu^{3+} < 0.1. This shows that in the competitive environment of the IBF droplet, the more abundant complexes are formed from the metals having larger ionic radii, which in turn suggests that the complexes involving the lighter
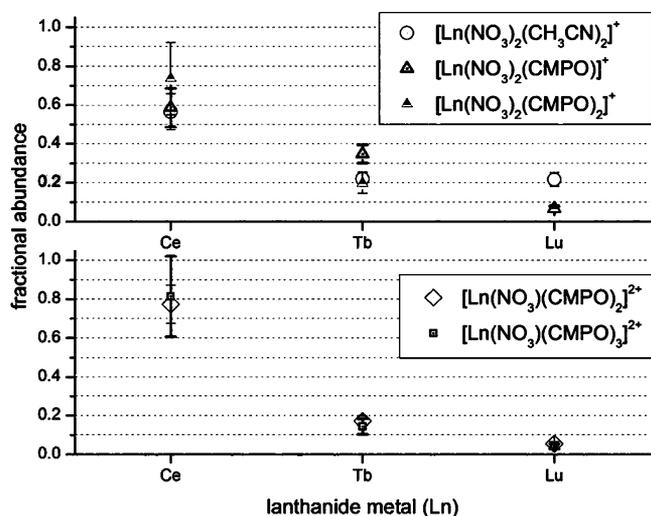
Figure 8. Fractional abundance (fa) values for lanthanide coordination complexes containing Ce^{3+}, Tb^{3+}, and Lu^{3+}. Top, 1+ complexes. Bottom, 2+ complexes.

lanthanides are more stable. We note that Chapon and co-workers concluded that the lighter lanthanides formed more stable complexes with amino-inositol ligands,[12h] and that Crowe observed higher dissociation energies for the nitrato,CMPO complexes of the lighter lanthanides.[14] Conversely, Colette and co-workers noted increasing conditional stability constants going from La^{3+} to Lu^{3+} for triazinyl,pyridinyl-type ligands using ESI-MS.[12k]

CONCLUSIONS

The efficiency of analyte transfer from sample solution to the mass spectrometer in electrospray ionization is typically a very small fraction. This attribute can create less-than-desirable analytical operations if there is only a very small quantity of analyte, or if the analyte possesses hazardous properties that would compromise safety when servicing the ESI source. In the present experiments, sample introduction having very high transfer efficiency was achieved using an induction-based fluidics device, which functions by launching single droplets from the end of a capillary directly into the ESI aperture of the mass spectrometer. The experimental setup enabled acquisition of positive and negative ion mass spectra of lanthanide nitrate solutions amended with a complexing ligand (CMPO) used in the solvent extraction processes, where the samples can be quite radioactive. The fact that apparently the entire sample is transferred into the mass spectrometer suggests that radiological control problems derived from loose contamination in the source region can be largely mitigated, which would enable a much broader suite of analyses for samples having this type of hazard.

The fact that all of the sample is transferred to the mass spectrometer also suggests that the measurement sensitivity in terms of analytical signal per mole of analyte consumed could be significantly higher than in the case of conventional ESI. Of course, transfer of solute into the mass spectrometer is only one part of the process; however, it is a step that has traditionally suffered from low efficiency. There is uncertainty regarding the nature of the droplets produced by IBF, specifically that droplet size may be significantly larger compared to conventional electrospray approaches leading to poorer ion production efficiency. Yet it is noted that experimentally the volume

dispensed from the pump is actually less than physically delivered to the mass spectrometer due to evaporation, and it has been shown that nanoliter droplets of various solutions have picocolumb charges,[3] similar to electrospray. In addition, we note that the mass spectra observed via IBF were in very good agreement with those generated using normal electrospray ionization,[9a] leading us to the opinion that the efficiency of ion production from droplets produced by IBF is probably similar to that of electrospray. These hypotheses are presently being investigated by additional studies, and preliminary results indicate that very low quantities of organics can be measured in single nanoliter droplets, provided the duty cycle of the mass spectrometer is sufficiently fast, or ion trapping is properly synchronized with droplet launching.

ASSOCIATED CONTENT

Ⓢ Supporting Information

Additional information as noted in the text. This material is available free of charge via the Internet at http://pubs.acs.org.

AUTHOR INFORMATION

Corresponding Author

*Phone: 208 526 2803. E-mail: gary.groenewold@inl.gov.

Notes

The authors declare no competing financial interest.

ACKNOWLEDGMENTS

REFERENCES

(1) (a) Jeannot, M. A.; Przyjazny, A.; Kokosa, J. M. *J. Chromatogr., A* **2010**, *1217*, 2326−2336. (b) Jain, A.; Verma, K. K. *Anal. Chim. Acta* **2011**, *706*, 37−65.

(2) Tu, T.; Sauter, A. D., Jr.; Sauter, A. D., III; Gross, M. L. *J. Am. Soc. Mass Spectrom.* **2008**, *19*, 1086−1090.

(3) Hilker, B.; Clifford, K. J.; Sauter, A. D., Jr.; Sauter, A. D., III; Harmon, J. P. *J. Am. Soc. Mass Spectrom.* **2009**, *20*, 1064−1067.

(4) Rayleigh, F. R. S. *Proc. London Math. Soc.* **1878**, *10*, 4−13.

(5) Elmqvist, R. Measuring Instrument of the Recording Type. United States Patent 2,566,443, Sep 4, 1951.

(6) Hilker, B.; Clifford, K. J.; Sauter, A. D., Jr.; Sauter, A. D., III; Gauthier, T.; Harmon, J. P. *Polymer* **2009**, *50*, 1015−1024.

(7) Jarecki, J. L.; Andersen, K.; Konop, C. J.; Knickelbine, J. J.; Vestling, M. M.; Stretton, A. O. *ACS Chem. Neurosci.* **2010**, *1*, 505−519.

(8) Brewer, T. M.; Szakal, C.; Gillen, G. *Rapid Commun. Mass Spectrom.* **2010**, 593−598.

(9) (a) Sauter, A. D.; Grange, G. A. Presented at the 59th Annual Meeting of the American Society of Mass Spectrometry; American Society for Mass Spectrometry: Denver, CO, 2011. (b) Sauter, A. D.; Scheeline, A.Presented at the 60th Annual Meeting of the American Society of Mass Spectrometry; American Society for Mass Spectrometry: Vancouver, Canada, 2012. (c) Sauter, A. D.; III, Sauter, A. D. Presented at the 60th Annual Meeting of the American Society of Mass Spectrometry; American Society for Mass Spectrometry: Vancouver, Canada, 2012.

(10) Fenn, J. B.; Mann, M.; Meng, C. K.; Wong, S. F.; Whitehouse, C. M. *Science* **1989**, *246*, 64−71.

(11) (a) Di Marco, V. B.; Bombi, G. G. *Mass Spectrom. Rev.* **2006**, *25*, 347−379. (b) Gatlin, L. C.; Turecek, F. *Electrospray Ionization Mass Spectrometry; Fundamentals, Instrumentation, and Applications*; Cole, R.

B., Ed.; John Wiley: New York, 1997, pp 527−570. (c) Keith-Roach, M. J. *Anal. Chim. Acta* **2010**, *678*, 140−148. (d) Stewart, I. I. *Spectrochim. Acta, Part B* **1999**, *54*, 1649−1695. (e) Groenewold, G. S. *Elemental and Isotope Ratio Mass Spectrometry*; Beauchemin, D.; Matthews, D. E., Ed.; Elsevier: Amsterdam, 2010; Vol. 5, pp 361−369. (f) Traeger, J. C. *Elemental and Isotope Ratio Mass Spectrometry*; Beauchemin, D.; Matthews, D. E., Ed.; Elsevier: Amsterdam, 2010; Vol. 5, pp 369−379. (g) Jirasko, R.; Holcapek, M. *Mass Spectrom. Rev.* **2011**, *30*, 1013−1036.

(12) (a) Stewart, I. I.; Horlick, G. *Anal. Chem.* **1994**, *66*, 3983−3993. (b) Platt, A. W. G.; Fawcett, J.; Hughes, R. S.; Russell, D. R. *Inorg. Chim. Acta* **1999**, *295*, 146−152. (c) Curtis, J. M.; Derrick, P. J.; Schnell, A.; Constantin, E.; Gallagher, R. T.; Chapman, J. R. *Inorg. Chim. Acta* **1992**, *201*, 197−201. (d) Colton, R.; Klaui, W. *Inorg. Chim. Acta* **1993**, *211*, 235−242. (e) Jackson, G. P.; King, F. L.; Goeringer, D. E.; Duckworth, D. C. *J. Phys. Chem. A* **2002**, *106*, 7788−7794. (f) Beer, P. D.; Brindley, G. D.; Fox, O. D.; Grieve, A.; Ogden, M. I.; Szemes, F.; Drew, M. G. D. *J. Chem. Soc., Dalton Trans.* **2002**, 3101−3111. (g) Lees, A. M. J.; Charnock, J. M.; Kresinski, R. W.; Platt, A. W. G. *Inorg. Chim. Acta* **2001**, *312*, 170−182. (h) Chapon, D.; Husson, C.; Delangle, P.; Lebrun, C.; Vottero, P. J. A. *J. Alloys Compd.* **2001**, *323*, 128−132. (i) Zhang, J. J.; Zhang, W.; Luo, Q. H.; Mei, Y. H. *Polyhedron* **1999**, *18*, 3637−3642. (j) Colette, S.; Amekraz, B.; Madic, C.; Berthon, L.; Cote, G.; Moulin, C. *Inorg. Chem.* **2002**, *41*, 7031−7041. (k) Colette, S.; Amekraz, B.; Madic, C.; Berthon, L.; Cote, G.; Moulin, C. *Inorg. Chem.* **2003**, *42*, 2215−2226. (l) Lau, R. L. C.; Jiang, J. Z.; Ng, D. K. P.; Chan, T. W. D. *J. Am. Soc. Mass Spectrom.* **1997**, *8*, 161−169. (m) Evans, W. J.; Johnston, M. A.; Fujimoto, C. H.; Greaves, J. *Organometallics* **2000**, *19*, 4258−4265. (n) Moulin, C.; Amekraz, B.; Colette, S.; Doizi, D.; Jacopin, C.; Lamouroux, C.; Plancque, G. *J. Alloys Compd.* **2006**, *408*, 1242−1245.

(13) (a) Ansari, S. A.; Pathak, P.; Mohapatra, P. K.; Manchanda, V. K. *Sep. Purif. Rev.* **2011**, *40*, 43−76. (b) Arai, K.; Yamashita, M.; Hatta, M.; Tomiyasu, H.; Ikeda, Y. *J. Nucl. Sci. Technol.* **1997**, *34*, 521−526. (c) Chitnis, R. R.; Wattal, P. K.; Ramanujam, A.; Dhami, P. S.; Gopalakrishnan, V.; Bauri, A. K.; Banerji, A. *J. Radioanal. Nucl. Chem.* **1999**, *240*, 721−726. (d) Horwitz, E. P.; Diamond, H.; Martin, K. A.; Chiarizia, R. *Solvent Extr. Ion Exch.* **1987**, *5*, 419−446. (e) Horwitz, E. P.; Kalina, D. G.; Diamond, H.; Vandegrift, G. F.; Schulz, W. W. *Solvent Extr. Ion Exch.* **1985**, *3*, 75−109. (f) Mathur, J. N.; Murali, M. S.; Nash, K. L. *Solvent Extr. Ion Exch.* **2001**, *19*, 357−390. (g) Murali, M. S.; Mathur, J. N. *Solvent Extr. Ion Exch.* **2001**, *19*, 61−77. (h) Schulz, W. W.; Horwitz, E. P. *Sep. Sci. Technol.* **1988**, *23*, 1191−1210.

(14) Crowe, M. C.; Kapoor, R. N.; Cervantes-Lee, F.; Parkanyi, L.; Schulte, L.; Pannell, K. H.; Brodbelt, J. S. *Inorg. Chem.* **2005**, *44*, 6415−6424.

(15) (a) Sauter, A. D. Precise Electrokinetic Delivery of Minute Volumes of Liquids. United States Patent 6,149,815, Nov 21, 2000. (b) Hantschel, T.; Fork, D. K.; Chow, E. M.; De Bruyker, D.; Rosa., M. A. Capillary-Channel Probes for Liquid Pickup, Transportation and Dispense Using Stressy Metal. United States Patent 7,749,448 B2, Jul 6, 2010. (c) United States Patent pending applications 60/574,104, 60/759,787, 60/881,532, 61/011,178, 61/797,060 and not yet assigned.